Combining the augmented Lagrangian preconditioner withe the SIMPLE Schur complement approximation

He, X.; Vuik, C.; Klaij, C.M.

Publication date
2017

Citation (APA)
He, X., Vuik, C., & Klaij, C. M. (2017). *Combining the augmented Lagrangian preconditioner withe the SIMPLE Schur complement approximation*. (Reports of the Delft Institute of Applied Mathematics; Vol. 17-06). Delft University of Technology.

DELFT UNIVERSITY OF TECHNOLOGY

REPORT 17-06

Combining the augmented Lagrangian preconditioner with the SIMPLE Schur complement approximation

X. He, C. Vuik and C.M. Klaij

ISSN 1389-6520

Reports of the Delft Institute of Applied Mathematics

Delft 2017

Abstract

The augmented Lagrangian (AL) preconditioner and its variant have been successfully applied to solve saddle point systems arising from the incompressible Navier-Stokes equations discretized by the finite element method. Attractive features are the purely algebraic construction and robustness with respect to the Reynolds number and mesh refinement. In this report, we reconsider the application of the AL preconditioner in the context of the stabilized finite volume methods and present the extension to the Reynolds-Averaged Navier-Stokes (RANS) equations, which are used to model turbulent flows in industrial applications. Furthermore, we propose a new variant of the AL preconditioner, obtained by substituting the approximation of the Schur complement from the SIMPLE preconditioner into the inverse of the Schur complement for the AL preconditioner. This new variant is applied to both Navier-Stokes and RANS equations to compute laminar and turbulent boundary-layer flows on grids with large aspect ratios. Spectral analysis shows that the new variant yields a more clustered spectrum of eigenvalues away from zero, which explains why it outperforms the existing variants in terms of the number of the Krylov subspace iterations.

Mathematics subject classification: 65F10, 65F08.

Keywords: Reynolds-Averaged Navier-Stokes equations, finite volume method, Block structured preconditioner, augmented Lagrangian preconditioner.

1 Introduction

The augmented Lagrangian (AL) preconditioner [3], belonging to the class of block structured preconditioners [8, 21, 22], is originally proposed to solve saddle point systems arising from the incompressible Navier-Stokes equations discretized by the finite element method (FEM). The AL preconditioner features a purely algebraic construction and the robustness with respect to the Reynolds number and mesh refinement. Because of these attractive features, recent research was devoted to the further development and extension of the AL preconditioner, notably the modified variants [4–6] with reduced computational complexity and the extension [27] to the context of stabilized finite volume methods (FVM), which are widely used in industrial computational fluid dynamic (CFD) applications.

Although applying FEM and FVM to the incompressible Navier-Stokes equations both leads to saddle point systems, the extension from FEM to FVM is nontrivial, see [27] for a detailed discussion on the dimensionless parameter that is involved in the AL preconditioner, its influence on the convergence of both nonlinear and linear iterations and the proposed rule to choose the optimal value in

practice. We did find that the features of the AL preconditioner exhibited in the FEM context, e.g. the robustness with respect to the Reynolds number and mesh refinement, are maintained in the context of FVM, at least for academic benchmarks. This motivates us to consider the application of the AL preconditioner in the broader context of Reynolds-Averaged Navier-Stokes (RANS) equations, which are used to model turbulent flows in industrial CFD applications. These equations are obtained by applying the Reynolds averaging process to the Navier-Stokes equations and adding an eddy-viscosity turbulence model to close the system, see [9, 17, 25]. Such models represent the effect of turbulence on the averaged flow quantities through a locally increased viscosity.

Unfortunately, straightforward application of the AL preconditioner to the RANS equations yields disappointing results as we will show in this report. Therefore, we reconsider the approximation of the Schur complement which is the key to the efficient block structured preconditioners [1, 2, 18]. In [12], we compared the exact Schur preconditioner with several cheaper approximations, including SIMPLE, for three test cases from maritime engineering, characterized by the thin turbulent boundary layers on grids with high aspect ratios. In this report, we propose a new Schur complement approximation which leads to a variant of the AL preconditioner. The approach is to substitute the approximation of the Schur complement from the SIMPLE preconditioner [11, 13] into the inverse of the Schur complement for the AL preconditioner. As we will show, the new variant of the AL preconditioner significantly speeds up the convergence rate of the Krylov subspace solvers for both turbulent and laminar boundary-layer flows computed with a stabilized FVM.

The structure of this report is as follows. The Reynolds-Averaged Navier-Stokes equations and the discretization and solution methods are introduced in Section 2. The new method to construct the approximation of the Schur complement in the AL preconditioner is presented in Section 3, followed by an analysis of the old approach. A comparison with the SIMPLE preconditioner in Section 4 is based on a basic cost model presented in Section 5. Section 6 includes the numerical experiments carried out on the turbulent and laminar benchmarks. Conclusions and future work are outlined in Section 7.

2 Governing equations and solution techniques

In this section, we introduce the Reynolds-Averaged Navier-Stokes equations as well as the finite volume discretization and solution methods.

2.1 Reynolds-Averaged Navier-Stokes equations

Incompressible, turbulent flows often occur in the CFD applications of the maritime industry. Most commercial and open-source CFD packages rely on the Reynolds-Averaged Navier-Stokes (RANS) equations to model such flows [9,17,25] since more advanced models, such as the Large-Eddy Simulation (LES), are still too expensive for industrial applications. Besides, engineers are firstly interested in the averaged properties of a flow, such as the average forces on a body, which is exactly what RANS models provide.

The RANS equations are obtained from the Navier-Stokes equations by an averaging process referred to as the Reynolds averaging, where an instantaneous quantity such as the velocity, is decomposed into its averaged and fluctuating part. If the flow is statistically steady, time averaging is used and ensemble averaging is applied for unsteady flows. The averaged part is solved for, while the fluctuating part is modelled which requires additional equations, for instance for the turbulent kinetic energy and turbulence dissipation, see [9, 17, 25] for a broader discussion. The Reynolds-Averaged momentum and continuity equations are here presented in the conservative form using FVM for a control volume Ω with surface S and outward normal vector $\mathbf{n}$:

$$\begin{aligned} \int_S \rho \mathbf{u}\mathbf{u}\cdot\mathbf{n}\,dS + \int_S P\mathbf{n}\,dS - \int_S \mu_{\text{eff}}(\nabla\mathbf{u}+\nabla\mathbf{u}^T)\cdot\mathbf{n}\,dS = \int_\Omega \rho\mathbf{b}\,d\Omega, \\ \int_S \mathbf{u}\cdot\mathbf{n}\,dS = 0 \end{aligned} \tag{1}$$

where $\mathbf{u}$ is the velocity, $P = p + \frac{2}{3}\rho k$ consists of the pressure p and the turbulent kinetic energy k , ρ is the (constant) density, μ_{eff} is the (variable) effective viscosity and $\mathbf{b}$ is a given force field. On the boundaries we either impose the velocity ($\mathbf{u} = \mathbf{u}_{\text{ref}}$ on inflow and $\mathbf{u} = 0$ on walls) or the normal stress ($\mu_{\text{eff}}\frac{\partial\mathbf{u}}{\partial\mathbf{n}} - P\mathbf{n} = 0$ on outflow and farfield). The effective viscosity μ_{eff} is the sum of the constant dynamic viscosity μ and the variable turbulent eddy viscosity μ_{t} provided by the turbulence model as a function of k and possibly of other turbulence quantities. Notice that for laminar flows, where k and μ_{t} are zero, the RANS equations reduce to the Navier-Stokes equations.

In this report, we will consider laminar flow of water over a finite flat plate at $\text{Re} = 10^5$ and turbulent flow at $\text{Re} = 10^7$. The density and dynamic viscosity of water at atmospheric pressure and 20 degrees Celsius are roughly $\rho = 1000[kg/m^3]$ and $\mu = 0.001[kg/m/s]$, see [26]. The inflow velocity $\mathbf{u}_{\text{ref}}$ in $[m/s]$ is adjusted to obtain the given Reynolds number $\text{Re} = \frac{\rho\|\mathbf{u}_{\text{ref}}\|L_{\text{ref}}}{\mu}$ based on the length $L_{\text{ref}} = 1[m]$ of the plate. The flow is characterized by a very thin boundary layer on the plate which is fully resolved by stretching the grid in the normal direction. This inevitably results in high aspect-ratio cells near the plate. At the higher Reynolds

number, the flow becomes turbulent in this thin boundary layer and in the wake of the plate. Figure 1 illustrates how the effective viscosity (provided in this case by the k-ω SST model) varies in the domain: the eddy viscosity in the wake of the plate is two orders of magnitude larger than the dynamic viscosity.

Solvers for the RANS equations should be able to handle both challenges, i.e. high-aspect ratio cells and significant variation in viscosity.

Figure 1: For the turbulent flat plate problem, the ratio between the eddy viscosity and dynamic viscosity, i.e., μ_t/μ in the wake of the plate.

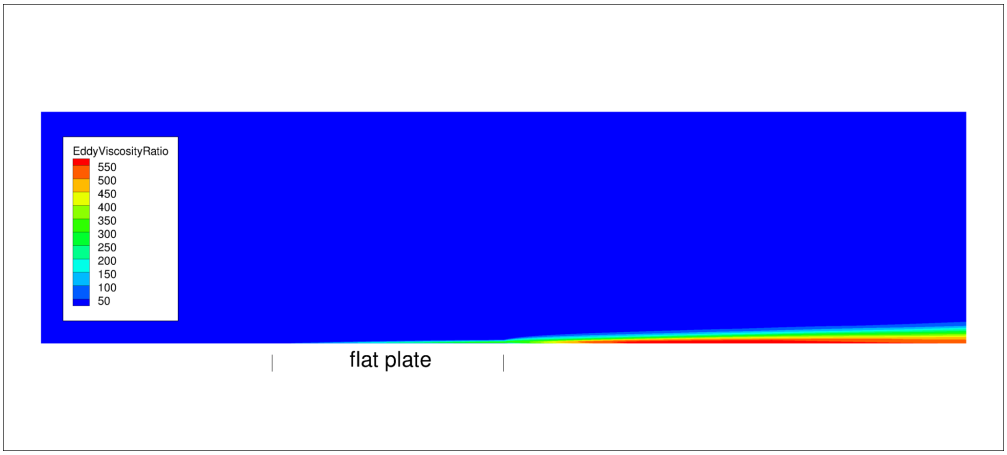

2.2 Linear saddle point system

As explained in [12], the nonlinear system (1) is solved for $\mathbf{u}$ and P as a series of linear systems obtained by Picard linearization [8], i.e. by assuming that the mass flux $\rho\mathbf{u}\cdot\mathbf{n}$, the turbulent kinetic energy k and the effective viscosity μ_{eff} are known from the previous iteration. The turbulence equations are then solved for k and possibly other turbulence quantities, after which the process is repeated until a convergence criterion is met.

After linearization and discretization of system (1) by the cell-centered and co-located FVM [9], the linear system is in saddle point form as

$$\begin{bmatrix} Q & G \\ D & C \end{bmatrix} \begin{bmatrix} \mathbf{u} \\ p \end{bmatrix} = \begin{bmatrix} \mathbf{f} \\ g \end{bmatrix} \quad \text{with} \quad \mathcal{A} := \begin{bmatrix} Q & G \\ D & C \end{bmatrix}, \tag{2}$$

where Q corresponds to the convection-diffusion operator and the matrices G and D denote the gradient and divergence operators, respectively. The matrix C comes from the stabilization method. The details of these matrices are presented as follows.

The linearization and the explicit treatment of the second diffusion term $\mu_{\text{eff}}\nabla\mathbf{u}^T\cdot\mathbf{n}$ by using the velocity and effective viscosity from the previous iteration make the

matrix Q of a block diagonal form. Each diagonal part Q_{ii} is equal and contains the contributions from the convective term $\rho u_i \mathbf{u} \cdot \mathbf{n}$ and the remaining diffusion term $\mu_{\text{eff}} \nabla u_i \cdot \mathbf{n}$.

In FEM the divergence matrix is the negative transpose of the gradient matrix, i.e. $D = -G^T$. However, in FVM we have $D_i = G_i$ on structured and unstructured grids, where i denotes the components therein. Only for structured grids we have that D is skew-symmetric ($D_i = -D_i^T$) and therefore that $D = -G^T$ as in FEM. We refer to [9] for the details of D and G in FVM.

To avoid pressure oscillations when the velocity and pressure are co-located in the cell centers, the pressure-weighted interpolation (PWI) method [16] is applied here and leads to the stabilization matrix C as

$$C = D\text{diag}^{-1}(Q)G - \text{diag}^{-1}(Q_{ii})L_p, \tag{3}$$

where L_p is the Laplacian matrix. The details about the PWI method and its representation by the discrete matrices as (3) are given in [11, 13].

2.3 Preconditioners for saddle point systems

Block structured preconditioners are used to accelerate the convergence rate of the Krylov subspace solvers for saddle point systems as (2). They are based on the block $\mathcal{LDU}$ decomposition of the coefficient matrix given by

$$\mathcal{A} = \mathcal{LDU} = \begin{bmatrix} Q & G \\ D & C \end{bmatrix} = \begin{bmatrix} I & O \\ DQ^{-1} & I \end{bmatrix} \begin{bmatrix} Q & O \\ O & S \end{bmatrix} \begin{bmatrix} I & Q^{-1}G \\ O & I \end{bmatrix}, \tag{4}$$

where $S = C - DQ^{-1}G$ is the so-called Schur complement. To successfully design block structured preconditioners, a combination of this block factorization with a suitable approximation of the Schur complement is utilized. It is not practical to explicitly form the exact Schur complement due to the action of Q^{-1} typically when the size is large. This implies that constructing the spectrally equivalent and numerically cheap approximations of the Schur complement can be very challenging. There exist several state-of-the-art approximations of the Schur complement, e.g. the least-square commutator (LSC) [7], pressure convection-diffusion (PCD) operator [10, 23], SIMPLE(R) preconditioner [13, 14, 24], and augmented Lagrangian (AL) approach [3–5, 27] etc. These Schur complement approximations are originally designed in the context of stable FEM where the $(2, 2)$ block of $\mathcal{A}$ is zero. We refer for more details of the Schur approximation to the surveys [1, 2, 18, 21, 22] and the books [8, 20].

This report is meant to significantly improve the efficiency of the AL preconditioner in the turbulent and laminar boundary-layer flows computed with a

stabilized FVM. To fulfill the objective of this report, a new variant of the AL preconditioner is proposed, which substitutes the approximation of the Schur complement from the SIMPLE preconditioner into the inverse of the Schur complement for the AL preconditioner. More details are presented in the next section.

3 Augmented Lagrangian preconditioner

In this section, we propose the new method to construct the approximation of the Schur complement in the AL preconditioner, followed by the analysis of and the comparison with the old approach.

3.1 Transformation of the linear system

To apply the AL preconditioner, the original system (2) is transformed into an equivalent one with the same solution [3, 5, 27], which is of the form

$$\begin{bmatrix} Q_\gamma & G_\gamma \\ D & C \end{bmatrix} \begin{bmatrix} \mathbf{u} \\ p \end{bmatrix} = \begin{bmatrix} \mathbf{f}_\gamma \\ g \end{bmatrix} \quad \text{with} \quad \mathcal{A}_\gamma := \begin{bmatrix} Q_\gamma & G_\gamma \\ D & C \end{bmatrix}, \tag{5}$$

where $Q_\gamma = Q - \gamma G W^{-1} D$, $G_\gamma = G - \gamma G W^{-1} C$ and $\mathbf{f}_\gamma = \mathbf{f} - \gamma G W^{-1} g$. The scalar $\gamma > 0$ and the matrix W should be non-singular. This transformation is obtained by multiplying $-\gamma G W^{-1}$ on both sides of the second row of system (2) and adding the resulting equation to the first one. Clearly, the transformed system (5) has the same solution as system (2) for any value of γ and any non-singular matrix W. The Schur complement of $\mathcal{A}_\gamma$ is $S_\gamma = C - D Q_\gamma^{-1} G_\gamma$.

The equivalent system (5) is what we want to solve when applying the AL preconditioner. Using the block $\mathcal{DU}$ decomposition of $\mathcal{A}_\gamma$, the ideal AL preconditioner $\mathcal{P}_{IAL}$ is given by

$$\mathcal{P}_{IAL} = \begin{bmatrix} Q_\gamma & G_\gamma \\ O & \widetilde{S}_\gamma \end{bmatrix}, \tag{6}$$

where $\widetilde{S}_\gamma$ denotes the approximation of S_γ.

The modified variant of the ideal AL preconditioner, i.e., the so-called modified AL preconditioner, replaces Q_γ by its block lower-triangular part, i.e. $\widetilde{Q}_\gamma$, such that the difficulty of solving sub-systems with Q_γ is avoided [27]. To see it more clearly, we take a 2D case as an example and give Q_γ and $\widetilde{Q}_\gamma$ as follows

$$Q = \begin{bmatrix} Q_1 & O \\ O & Q_1 \end{bmatrix}, G = \begin{bmatrix} G_1 \\ G_2 \end{bmatrix}, D = \begin{bmatrix} D_1 & D_2 \end{bmatrix},$$

$$Q_\gamma = \begin{bmatrix} Q_1 - \gamma G_1 W^{-1} D_1 & -\gamma G_1 W^{-1} D_2 \\ -\gamma G_2 W^{-1} D_1 & Q_1 - \gamma G_2 W^{-1} D_2 \end{bmatrix}, \widetilde{Q}_\gamma = \begin{bmatrix} Q_1 - \gamma G_1 W^{-1} D_1 & O \\ -\gamma G_2 W^{-1} D_1 & Q_1 - \gamma G_2 W^{-1} D_2 \end{bmatrix}.$$

Substituting $\widetilde{Q}_\gamma$ into $\mathcal{P}_{IAL}$ as (6), then we get the modified AL preconditioner $\mathcal{P}_{MAL}$:

$$\mathcal{P}_{MAL} = \begin{bmatrix} \widetilde{Q}_\gamma & G_\gamma \\ O & \widetilde{S}_\gamma \end{bmatrix}. \tag{7}$$

It appears that one needs to solve sub-systems with $\widetilde{Q}_\gamma$ when applying $\mathcal{P}_{MAL}$. This work is further reduced to solve systems with $Q_1 - \gamma G_1 W^{-1} D_1$ and $Q_1 - \gamma G_2 W^{-1} D_2$. These two sub-blocks do not contain the coupling between two components of the velocity so that it is much easier to solve, compared to Q_γ involved in $\mathcal{P}_{IAL}$.

3.2 New Schur complement approximation

The key of the ideal and modified AL preconditioners is to find a numerically cheap and spectrally equivalent Schur complement approximation $\widetilde{S}_\gamma$. The novel approximation proposed by this report is based on the following lemma.

Lemma 3.1 *Assuming that all the relevant matrices are invertible, then the inverse of S_γ is given by*

$$S_\gamma^{-1} = S^{-1}(I - \gamma C W^{-1}) + \gamma W^{-1}, \tag{8}$$

where $S = C - DQ^{-1}G$ denotes the Schur complement of the original system (2).

Proof. We refer to [27] for the proof. ∎

This lemma was already published but its importance was not fully appreciated. Since Lemma 3.1 gives the connection between the Schur complement S_γ and S, it provides a framework to build the approximation of S_γ. Provided an approximation of S denoted by $\widetilde{S}$, it is natural to substitute $\widetilde{S}$ into expression (8) to construct an approximation of S_γ in the inverse form as

$$\widetilde{S}_{\gamma\ \text{new}}^{-1} = \widetilde{S}^{-1}(I - \gamma C W^{-1}) + \gamma W^{-1}, \tag{9}$$

where the notation *new* is used to differ from the old approach to approximate S_γ, discussed in the next section.

Actually it is not necessary to explicitly implement $\widetilde{S}_{\gamma\ \text{new}}$. Solving a sub-system with $\widetilde{S}_{\gamma\ \text{new}}$, i.e., $\widetilde{S}_{\gamma\ \text{new}}\ \mathbf{x} = \mathbf{b}$, converts to multiply the vector $\mathbf{b}$ on both sides of expression (9). Supposed that W is a diagonal matrix, e.g. the mass matrix M_p with density multiplied with cell volumes in FVM, the complexity of $(\widetilde{S}^{-1}(I - \gamma C W^{-1}) + \gamma W^{-1})\mathbf{b}$ is focused on solving the system with $\widetilde{S}$. This means that the accelerating techniques to optimize $\widetilde{S}$ can reduce the computational time of the new approach.

From expression (9) it is clear that the Schur complement approximation $\widetilde{S}$ proposed for the original system (2) is used to construct $\widetilde{S}_{\gamma \text{ new}}$ here. Among the known LSC, PCD and SIMPLE methods, this report chooses the Schur complement approximation arising from the SIMPLE preconditioner. The main reason is that the LSC and PCD methods are applicable only to the stable FEM discretizations, see [7, 10, 23]. The extension to the stabilized FEM and FVM is not available and not trivial.

Regarding the Schur complement $S = C - DQ^{-1}G$ of the original system (2), the SIMPLE preconditioner approximates Q by its diagonal, $\text{diag}(Q)$, and obtains the approximation of S as $\widetilde{S}_1 = C - D\text{diag}^{-1}(Q)G$. Taking into account the stabilization matrix $C = D\text{diag}^{-1}(Q)G - \text{diag}^{-1}(Q_{ii})L_p$ as given in (3), we further reduce the approximation to $\widetilde{S}_{\text{SIMPLE}} = -\text{diag}^{-1}(Q_{ii})L_p$ because the term $D\text{diag}^{-1}(Q)G$ in $\widetilde{S}_1$ and C cancels. See, for instance, [11, 13] for a detailed discussion of obtaining $\widetilde{S}_{\text{SIMPLE}}$ in FVM. Substituting $\widetilde{S}_{\text{SIMPLE}}$ and $W = M_p$ into expression (9) we obtain

$$\widetilde{S}^{-1}_{\gamma \text{ new}} = \widetilde{S}^{-1}_{\text{SIMPLE}}(I - \gamma C M_p^{-1}) + \gamma M_p^{-1}, \text{ where } \widetilde{S}_{\text{SIMPLE}} = -\text{diag}^{-1}(Q_{ii})L_p. \quad (10)$$

Based on the above approach, it is seen that there is no extra requirement on the value of the parameter γ so that $\widetilde{S}_{\gamma \text{ new}}$ can be obtained. This is in contrast with the old Schur complement approximation presented in the next section, there the parameter γ plays an important role and it is contradictory to balance the value of γ so that the old Schur approximation and other essential assumptions can be simultaneously satisfied. This implies that the new Schur approximation exhibits an inherent advantage over the old one. Therefore, both the turbulent and laminar computations benefit from the new Schur approximation in terms of a much faster convergence rate of the Krylov subspace solvers. See the results in the numerical experiment section.

3.3 Old Schur complement approximation

For a comparison reason, the old approximation of the Schur complement in the AL preconditioner is analyzed in this section. The starting point to construct the old approximation of the Schur complement in the AL preconditioner is also Lemma 3.1. However, the strategy is totally different. Choosing $W_1 = \gamma C + M_p$ and substituting W_1 into expression (8) we have

$$\begin{aligned} S_\gamma^{-1} &= S^{-1}(I - (\gamma C + M_p - M_p)(\gamma C + M_p)^{-1}) + \gamma(\gamma C + M_p)^{-1} \\ &= S^{-1}M_p(\gamma C + M_p)^{-1} + \gamma(\gamma C + M_p)^{-1} \\ &= (\gamma^{-1}S^{-1}M_p + I)(C + \gamma^{-1}M_p)^{-1}. \end{aligned}$$

For large values of γ such that $\| \gamma^{-1} S^{-1} M_p \| \ll 1$ we can approximate S_γ by

$$\widetilde{S}_{\gamma \text{ old}} = C + \gamma^{-1} M_p. \tag{11}$$

The choice of $W_1 = \gamma C + M_p$ is not practical since the action of W_1^{-1} is needed in the transformed system (5). Considering the mass matrix M_p which is a diagonal matrix in FVM and omitting the term γC in W_1, the related references, for instance [4, 27], utilize $W = M_p$ and $\widetilde{S}_{\gamma \text{ old}}$ in the ideal and modified AL preconditioners.

The unavoidable disadvantage of the above method is presented as follows. The approximation $\widetilde{S}_{\gamma \text{ old}}$ is obtained if and only if $W_1 = \gamma C + M_p$ and large values of γ are chosen. However, $W = M_p$ is close to $W_1 = \gamma C + M_p$ only when γ is small. This means that it is contradictory to tune the value of γ so that $W = M_p$ and $\widetilde{S}_{\gamma \text{ old}}$ could be simultaneously obtained. A simply balanced value of γ is $\gamma = 1$ or $O(1)$. This disadvantage reflects in the convergence rate of the Krylov subspace solvers. This report shows that for the laminar calculations the number of the Krylov subspace iterations preconditioned by the AL preconditioner with $\widetilde{S}_{\gamma \text{ old}}$ is ten times larger than the new Schur approximation $\widetilde{S}_{\gamma \text{ new}}$. An application of the AL preconditioner with $\widetilde{S}_{\gamma \text{ old}}$ in the more challenging turbulent computations with variable viscosity and more stretched grids shows a very slow convergence or even stagnation. See numerical experiments in Section 6.

In summary, regarding the ideal and modified AL preconditioners applied to the transformed system (5), there are two types of Schur complement approximations, i.e.

1. $\widetilde{S}^{-1}_{\gamma \text{ new}} = \widetilde{S}^{-1}_{\text{SIMPLE}}(I - \gamma C M_p^{-1}) + \gamma M_p^{-1}, \quad \widetilde{S}_{\text{SIMPLE}} = -\text{diag}^{-1}(Q_{ii}) L_p.$
2. $\widetilde{S}_{\gamma \text{ old}} = C + \gamma^{-1} M_p.$

The choice of $W = M_p$ is fixed in the transformation to obtain the equivalent system (5) and the construction of two Schur complement approximations.

4 SIMPLE preconditioner

Although the focus of this report is on the new Schur complement approximation and its advantage over the old one in the AL preconditioner, we also present the SIMPLE preconditioner for a more comprehensive comparison. Different from the ideal AL preconditioner and its modified variant, the SIMPLE preconditioner is proposed for the original system (2), which is based on the block $\mathcal{LDU}$ decomposition of the coefficient matrix $\mathcal{A}$ and given by

$$\mathcal{P}_{SIMPLE} = \begin{bmatrix} Q & O \\ D & \widetilde{S} \end{bmatrix} \begin{bmatrix} I & \text{diag}^{-1}(Q) G \\ O & I \end{bmatrix},$$

where $\widetilde{S}$ denotes the approximation of the Schur complement of $\mathcal{A}$, i.e., $S = C - DQ^{-1}G$. Considering the stabilization matrix C in FVM, the Schur complement approximation is obtained as $\widetilde{S} = \widetilde{S}_{\text{SIMPLE}} = -\text{diag}^{-1}(Q_{ii})L_p$ where L_p is the Laplacian matrix. Therefore, the scaled Laplacian matrix is used as the approximation of the Schur complement in the SIMPLE preconditioner. In order to avoid repetition we refer to Section 3.2 for the details of obtaining $\widetilde{S}_{\text{SIMPLE}}$.

5 Cost model for AL and SIMPLE preconditioners

To summarize the linearized systems where the AL and SIMPLE preconditioners are applied individually, we give the schematic diagram as follows:

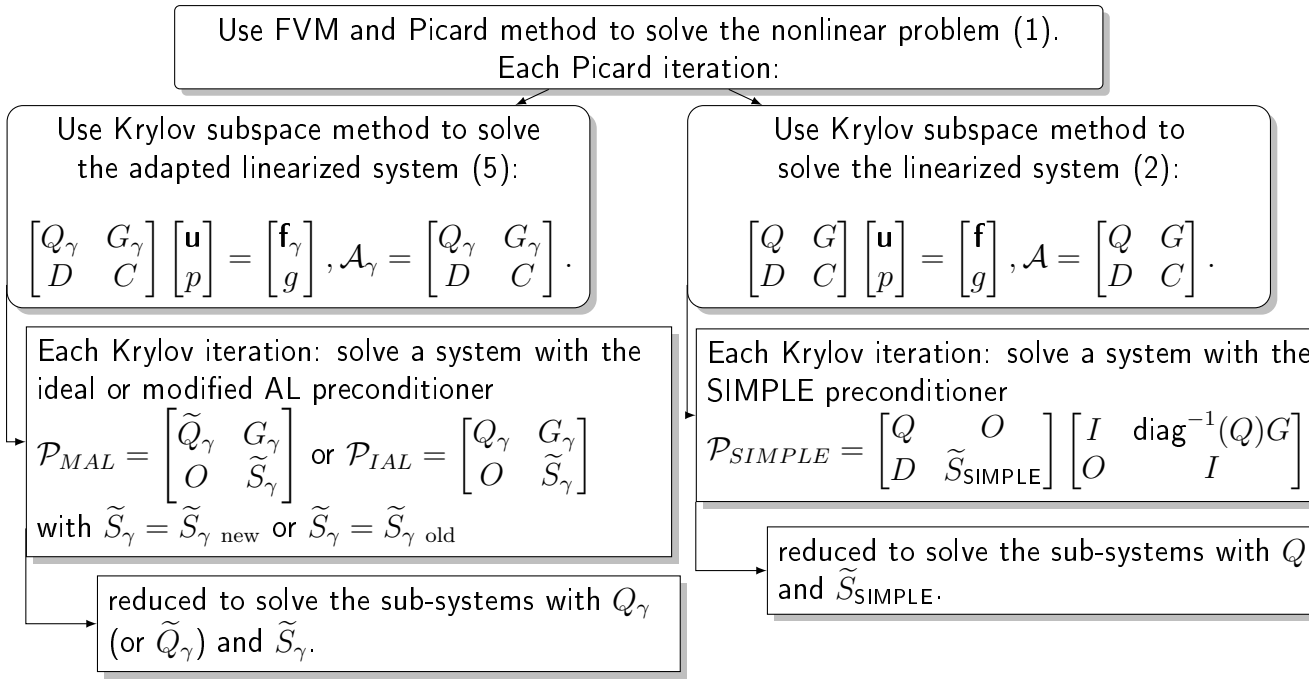

The application of the AL preconditioner is presented on the left side. The alternative, namely the SIMPLE preconditioner with the scaled Laplacian as the Schur approximation, is on the right side. At each Picard iteration, we choose one of the two linear systems to solve and employ the corresponding preconditioner. When choosing the AL preconditioner, there are two options, i.e., the ideal AL preconditioner and its variant - the modified AL preconditioner. The new Schur complement approximation $\widetilde{S}_{\gamma\ \text{new}}$ proposed in this report is applicable for both the ideal and modified AL preconditioners, the same as the old approximation $\widetilde{S}_{\gamma\ \text{old}}$.

In [12], we presented a basic cost model to discriminate between the SIMPLE preconditioner and other preconditioners. Here, we extend the model to include the

modified AL preconditioner with two Schur complement approximations. Firstly consider the cost of using the SIMPLE preconditioner $\mathcal{P}_{SIMPLE}$ for a Krylov subspace method that solves the system with $\mathcal{A}$ to a certain relative tolerance in n_1 iterations. The preconditioner is applied at each Krylov iteration and the SIMPLE preconditioner solves the momentum sub-system 'mom-u' with Q and the pressure sub-system 'mass-p' with $\widetilde{S}_{\text{SIMPLE}}$. Besides, at each Krylov iteration another cost is expressed in the product of the coefficient matrix $\mathcal{A}$ with a Krylov residual vector $\mathbf{b}_{res}$. Thus, the total cost is

- $\mathcal{P}_{SIMPLE}$: $\quad n_1 \times (\text{mom-u with } Q + \text{mass-p with } \widetilde{S}_{\text{SIMPLE}} + \mathcal{A} \times \mathbf{b}_{res})$.

Secondly consider the cost of applying the modified AL preconditioner $\mathcal{P}_{MAL}$ with the new Schur approximation $\widetilde{S}_{\gamma \text{ new}}$ for a Krylov subspace method that solves the transformed system with $\mathcal{A}_\gamma$ to a certain relative tolerance in n_2 iterations. The total cost consists of solving the momentum sub-system 'mom-u' with $\widetilde{Q}_\gamma$, the pressure sub-system 'mass-p' with $\widetilde{S}_{\gamma \text{ new}}$ and the matrix-vector product $\mathcal{A}_\gamma \times \mathbf{b}_{res}$. If we neglect the multiplications in the definition of $\widetilde{S}_{\gamma \text{ new}}$ as given in (10), the cost of solving the pressure sub-system with $\widetilde{S}_{\gamma \text{ new}}$ is the same as $\widetilde{S}_{\text{SIMPLE}}$. Thus, the total cost is

- $\mathcal{P}_{MAL}$ with $\widetilde{S}_{\gamma \text{ new}}$: $\quad n_2 \times (\text{mom-u with } \widetilde{Q}_\gamma + \text{mass-p with } \widetilde{S}_{\text{SIMPLE}} + \mathcal{A}_\gamma \times \mathbf{b}_{res})$.

To apply the modified AL preconditioner, the original system with $\mathcal{A}$ should be transformed to the equivalent one with $\mathcal{A}_\gamma$, which consumes an additional transformation cost at each Picard iteration. Compared with the time expressed on the solution process, the transformation is the secondary time consuming task so that the associated cost is not included in the presented cost model.

At each Krylov iteration, there are two resources leading to a higher cost of the modified AL preconditioner with the new Schur approximation, compared to the SIMPLE preconditioner. More nonzero fill-in is introduced in the blocks Q_γ and G_γ that increases the cost of matrix-vector product $\mathcal{A}_\gamma \times \mathbf{b}_{res}$. For the laminar flat plate problem, the nonzero entries in Q_γ and G_γ are about 5 times more than Q and G involved in $\mathcal{A}$, see [27] for the sparsity of the blocks. Besides, if we employ the Krylov subspace solver, the cost of solving the momentum sub-system with $\widetilde{Q}_\gamma$ is heavier than Q. The reasons are that the number of nonzero entries of $\widetilde{Q}_\gamma$ are more than Q and the condition number of $\widetilde{Q}_\gamma$ can increase due to the introduced term $-\gamma G W^{-1} D$. See [27] for the numerical comparison between solving the sub-systems with $\widetilde{Q}_\gamma$ and Q. Therefore, this higher cost of $\mathcal{P}_{MAL}$ with $\widetilde{S}_{\gamma \text{ new}}$ only pays-off if the number of the Krylov iterations n_2 is less than n_1 by applying the SIMPLE preconditioner.

Finally consider the cost of applying the modified AL preconditioner $\mathcal{P}_{MAL}$ with the old Schur approximation $\widetilde{S}_{\gamma\ \text{old}}$. Similar to the analysis of $\mathcal{P}_{MAL}$ with $\widetilde{S}_{\gamma\ \text{new}}$, we obtain the total cost as

- $\mathcal{P}_{MAL}$ with $\widetilde{S}_{\gamma\ \text{old}}$: $\quad n_3 \times (\text{mom-u with } \widetilde{Q}_\gamma + \text{mass-p with } \widetilde{S}_{\gamma\ \text{old}} + \mathcal{A}_\gamma \times \mathbf{b}_{res})$.

Clearly, the difference of cost by applying $\mathcal{P}_{MAL}$ with $\widetilde{S}_{\gamma\ \text{new}}$ and $\widetilde{S}_{\gamma\ \text{old}}$ arises from solving the pressure sub-systems with $\widetilde{S}_{\text{SIMPLE}}$ and $\widetilde{S}_{\gamma\ \text{old}}$, respectively. It is difficult to analytically compare the complexity of solving the sub-systems with $\widetilde{S}_{\text{SIMPLE}}$ and $\widetilde{S}_{\gamma\ \text{old}}$. However, numerical experiments in the next section show that the number of the Krylov subspace iterations preconditioned by $\mathcal{P}_{MAL}$ with $\widetilde{S}_{\gamma\ \text{new}}$ is significantly reduced compared to $\widetilde{S}_{\gamma\ \text{old}}$. This makes the new Schur complement approximation more efficient and attractive.

6 Numerical experiments

In this section, we compare the new AL variant with the old one and with SIMPLE preconditioner, for incompressible, laminar flow governed by the Navier-Stokes equations, as well as turbulent flow governed by the Reynolds-Averaged Navier-Stokes equations.

6.1 Flow over a finite flat plate

Flow over a finite flat plate is a standard test case in maritime engineering, see [19] for a detailed study of various turbulence models with MARIN's CFD software package ReFRESCO [15].

We first consider the fully turbulent flow at $\text{Re} = 10^7$ on the block-structured grids. The grids are refined near the leading and trailing edge of the plate and spread out in the wake of the plate, see Figure 2(a), which leads to some eccentricity and non-orthogonality. As can be seen, the grids are stretched in both the horizontal and vertical direction and reach the maximal aspect ratio of order $1 : 10^4$ near the middle of the plate. The complete flow is computed, starting from uniform laminar flow upstream of the plate.

Second, we reconsider laminar flow at $\text{Re} = 10^5$ on a straight single-block grid. This case was already presented in [11–13,27] for other solvers and preconditioners. We reconsider it here to show that the new Schur complement approximation also improves the efficiency of the AL preconditioner in the calculations of laminar flow. The stretched grids shown in Figure 2(b) are generated based on uniform Cartesian grids by applying the stretching function from [13] in the vertical direction. Near the plate the grids have a maximal aspect ratio of order $1 : 50$, which is about

two orders smaller than the turbulent grids. Contrary to the turbulent case, the flow starts with the (semi-analytical) Blasius solution halfway the plate, so only the second half and the wake are computed.

Figure 2: Impression of the grids. Turbulent case with 80×40 cells and the max aspect ratio of order $1 : 10^4$ and laminar case with 64×64 cells and the max aspect ratio of order $1 : 50$.

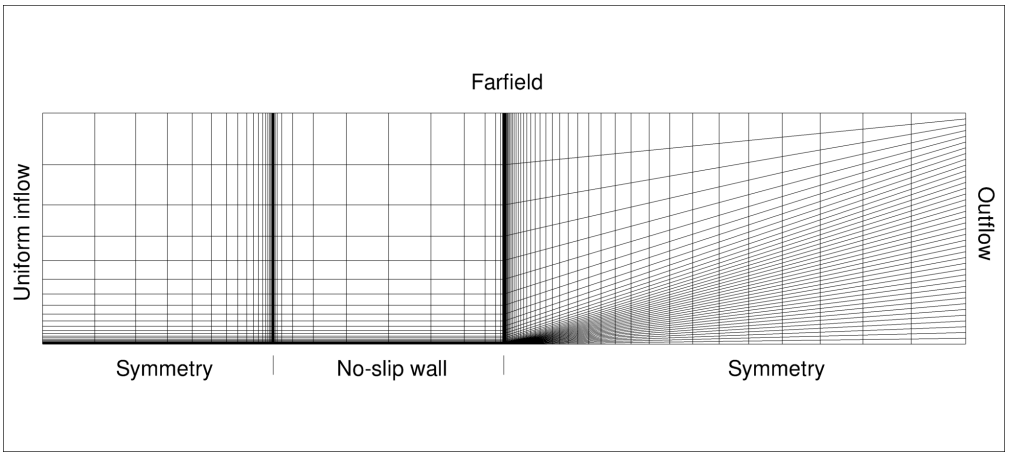

(a) Turbulent case

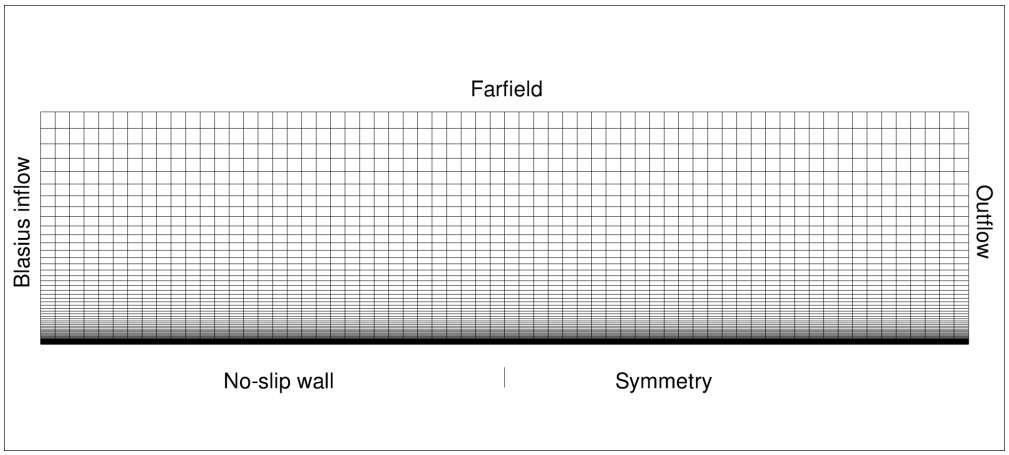

(b) Laminar case

In this report all experiments are carried out based on the blocks Q, G, D, C, M_p and L_p and the right hand-side vector rhs, which are obtained at the 30th nonlinear iteration with a 80×40 structured grid for the turbulent case and with a 64×64 structured grid for the laminar case. These blocks and rhs are generated by ReFRESCO and imported into Matlab. The aim of the numerical experiments is to show the variation in the eigenvalues and number of the Krylov subspace iterations, arising from different Schur complement approximations in

the AL preconditioner. To carry out a comprehensive evaluation of the new Schur complement approximation in the AL preconditioner, in this report we solve the linear system preconditioned by the AL preconditioner with the new Schur complement approximation to the machine accuracy. For a fair comparison, the same stopping tolerance is used when employing the old Schur complement approximation and the SIMPLE preconditioner. Since the AL preconditioner with different Schur complement approximations and the SIMPLE preconditioner involve various momentum or pressure sub-systems, all the sub-systems are directly solved in this report to avoid the sensitiveness of iterative solvers on the varying solution complexities.

6.2 Numerical experiments on the turbulent case

To find out the reason that the new Schur complement approximation $\widetilde{S}_{\gamma\ \text{new}}$ leads to a fast convergence of the Krylov subspace solvers preconditioned by the AL preconditioner, we plot ten extreme eigenvalues of the preconditioned matrices $\mathcal{P}_{IAL}^{-1}\mathcal{A}_\gamma$ and $\mathcal{P}_{MAL}^{-1}\mathcal{A}_\gamma$. The results are shown in Figure 3 and 4. Regarding the ideal AL preconditioner, results in Figure 3 show that the smallest eigenvalues are far away from zero and the spectrum is clustered due to a small ratio between the largest and smallest magnitude of eigenvalues. Such a distribution of eigenvalues is favorable for Krylov subspace solvers and a fast convergence rate can be expected. An analogous distribution of eigenvalues of $\mathcal{P}_{MAL}^{-1}\mathcal{A}_\gamma$ is observed in Figure 4.

The value of γ influences the distribution of eigenvalues as seen in Figure 3 and 4. For relative small values, e.g. $\gamma = 0.01$ and $\gamma = 1$ the effect is moderate. However, for $\gamma = 100$ the smallest eigenvalue of $\mathcal{P}_{MAL}^{-1}\mathcal{A}_\gamma$ is two orders of magnitude smaller than $\gamma = 0.01$ and $\gamma = 1.0$, see the last row of Figure 4. It appears that the optimal value of γ, which leads to the most clustered eigenvalues, is the same for both the ideal and modified AL preconditioners, i.e., $\gamma_{\text{opt}} = 1$.

Results in Figure 5 show the fast convergence rate of the Krylov subspace solver preconditioned by the ideal and modified AL preconditioners with the new Schur approximation $\widetilde{S}_{\gamma\ \text{new}}$. This conforms the prediction that the new Schur approximation $\widetilde{S}_{\gamma\ \text{new}}$ produces a favorable preconditioner for the Krylov subspace solvers. In Figure 5 we see that the convergence rate varies with various values of γ and $\gamma_{\text{opt}} = 1$ results in the fastest convergence. This again confirms the prediction regarding the effect of parameter γ.

The very slow convergence rate of the Krylov subspace solver preconditioned by the AL preconditioner with the old Schur complement approximation $\widetilde{S}_{\gamma\ \text{old}}$ and $\gamma = 1$ is shown in Figure 6. To understand this slow convergence the extreme eigenvalues are presented in Figure 7. We see that the smallest eigenvalues are quite close to zero for all tested values of γ, which degrades the efficiency of the

Krylov subspace solver considerably.

These numerical results clearly show that the new Schur complement approximation $\widetilde{S}_{\gamma\ \mathrm{new}}$ proposed in this report significantly improves the performance of the AL preconditioner for turbulent flows.

We also present the spectrum of eigenvalues and convergence rate by using the SIMPLE preconditioner. These results are compared with the modified AL preconditioner with the new Schur complement approximation $\widetilde{S}_{\gamma\ \mathrm{new}}$ and $\gamma_{\mathrm{opt}} = 1$. The comparison given in Figure 8 illustrates that the smallest eigenvalues are nearly the same for both preconditioners. However, the SIMPLE preconditioner leads to a larger ratio between the largest and smallest magnitude of eigenvalues, which means that the spectrum of eigenvalues is less clustered compared to the modified AL preconditioner. Therefore, a faster convergence rate of the Krylov subspace solver is expected and obtained by applying the modified AL preconditioner with the new Schur complement approximation $\widetilde{S}_{\gamma\ \mathrm{new}}$ and $\gamma_{\mathrm{opt}} = 1$, as seen in Figure 9. The number of the Krylov subspace iterations by applying the modified AL preconditioner with $\widetilde{S}_{\gamma\ \mathrm{new}}$ and $\gamma_{\mathrm{opt}} = 1$ is around 140 and is about 180 by employing the SIMPLE preconditioner.

6.3 Numerical experiments on the laminar case

Figure 10 plots ten extreme eigenvalues of $\mathcal{P}_{IAL}^{-1}\mathcal{A}_{\gamma}$ with the new Schur approximation $\widetilde{S}_{\gamma\ \mathrm{new}}$ for the laminar case. As seen the smallest eigenvalues are far away from zero and the ratio between the largest and smallest magnitude of eigenvalues is small. This means that the new Schur approximation $\widetilde{S}_{\gamma\ \mathrm{new}}$ also leads to a clustered spectrum in the laminar case. In Figure 10 we only present the results with $\gamma = 1$ the reason being that laminar experiments not shown here illustrate that the variation of the value of γ slightly effects the distribution of eigenvalues of $\mathcal{P}_{IAL}^{-1}\mathcal{A}_{\gamma}$ with the new Schur approximation $\widetilde{S}_{\gamma\ \mathrm{new}}$.

In practice the modified AL preconditioner is often utilize due to the reduced complexity of solving the sub-systems with $\widetilde{Q}_{\gamma}$, compared to Q_{γ} involved in the ideal AL preconditioner. The extreme eigenvalues of $\mathcal{P}_{MAL}^{-1}\mathcal{A}_{\gamma}$ with the new Schur approximation $\widetilde{S}_{\gamma\ \mathrm{new}}$ is shown in Figure 11. There are two observations to be made. Firstly, for moderate values of γ, e.g., $\gamma \in [0.01,\ 0.1]$, the smallest eigenvalues are far away from zero. Secondly, $\gamma = 0.1$ results in the smallest ratio between the largest and smallest magnitude of eigenvalues. Thus, it appears that the optimal value is $\gamma_{\mathrm{opt}} = 0.1$ for the laminar case. Considering $\gamma_{\mathrm{opt}} = 1$ for the turbulent case case, the optimal value of γ seems to lie in the interval $[0.1,\ 1]$.

Figure 12 shows the variation of the distribution of eigenvalues arising from different Schur complement approximations. We found in [27] that for the laminar case the optimal value of γ for the old Schur approximation $\widetilde{S}_{\gamma\ \mathrm{old}}$ is $\gamma_{\mathrm{opt}} = 400$. As

seen in Figure 12, the smallest eigenvalues with $\widetilde{S}_{\gamma\ \text{old}}$ and $\gamma_{\text{opt}} = 400$ are quite close to zero and about five orders of magnitude smaller than the new Schur approximation $\widetilde{S}_{\gamma\ \text{new}}$ and $\gamma_{\text{opt}} = 0.1$. Therefore, the new Schur complement approximation $\widetilde{S}_{\gamma\ \text{new}}$ can lead to a much faster convergence rate than the old Schur complement approximation $\widetilde{S}_{\gamma\ \text{old}}$. This is confirmed by the results shown in Figure 14.

Figure 13 compares the distribution of eigenvalues of the preconditioned matrix by applying the modified AL and SIMPLE preconditioners. It is seen that the modified AL preconditioner with the new Schur approximation $\widetilde{S}_{\gamma\ \text{new}}$ and $\gamma_{opt} = 0.1$ leads to a more clustered eigenvalues, compared to the SIMPLE preconditioner. Therefore, a faster convergence can be expected on the laminar case, which is confirmed by Figure 14.

Figure 14 presents the convergence rate of the Krylov subspace solvers by applying the modified AL preconditioner with two Schur approximations and the SIMPLE preconditioner. Clearly seen on the laminar case the modified AL preconditioner with the new Schur approximation $\widetilde{S}_{\gamma\ \text{new}}$ and $\gamma_{\text{opt}} = 0.1$ reduces the number of the Krylov subspace iterations by factors 10 and 1.9, compared to the old Schur approximation $\widetilde{S}_{\gamma\ \text{old}}$ with $\gamma_{opt} = 400$ and the SIMPLE preconditioner, respectively.

The above numerical results clearly show that the new Schur complement approximation $\widetilde{S}_{\gamma\ \text{new}}$ proposed in this report significantly improves the performance of the AL preconditioner for laminar flows too.

In the previous work [27] we set the stopping tolerance for the linear system to be 10^{-3} on the laminar FP case and compare the modified AL preconditioner with the old Schur complement approximation and the SIMPLE preconditioner in terms of the number of the Krylov subspace iterations. This comparison is executed based on the chosen stopping tolerance which balances the linear and nonlinear solvers. Since the nonlinear solver is not the focus of this report, it is reasonable to solve the linear system to the machine accuracy so that a comprehensive evaluation of the proposed new Schur complement approximation in the AL preconditioner and a complete comparison with the old Schur complement approximation and the SIMPLE preconditioner can be obtained. In this sense, the results in Figure 14, regarding the number of the Krylov subspace iterations preconditioned by the modified AL preconditioner with the old Schur complement approximation and the SIMPLE preconditioner, supplement the previous work [27].

Finally we put the turbulent and laminar results together for a comparison. Consider the modified AL preconditioner with the new Schur approximation and the optimal value of γ , it appears that the number of the Krylov subspace iterations is comparable for two cases, see results in Figures 9 and 14. This means that the new Schur complement approximation proposed in this report makes the AL preconditioner robust with respect to the mesh anisotropy and physical parameter

variation, e.g. the variation of the viscosity. Furthermore the value of γ_{opt} is much easier to determine for the new variant. Besides, the advantage of the new Schur approximation over the old one is clearly exhibited in terms of the significantly reduced number of the Krylov subspace iterations for both cases. This means that new Schur approximation can considerably improve the efficiency of the AL preconditioner for both turbulent and laminar calculations. Although the number of the Krylov subspace iterations by applying the modified AL preconditioner with new Schur approximation and the optimal value of γ is less than the SIMPLE preconditioner (see Figures 9 and 14), the benefit in terms of the total wall-clock time needs the further assessment due to the heavier cost of the AL preconditioner presented in Section 5. This is included in the future research plan.

7 Conclusion and future work

In this report, we have considered the extension of the AL preconditioner in the context of the stabilized finite volume methods to both laminar flow governed by the Navier-Stokes equations and turbulent flow governed by the Reynolds-Averaged Navier-Stokes (RANS) equations with eddy-viscosity turbulence model.

We find out that the straightforward application of the AL preconditioner to the RANS equations yields disappointing results and therefore proposed a new Schur complement approximation which leads to a variant of the AL preconditioner. The approach is to substitute the approximation of the Schur complement from the SIMPLE preconditioner into the inverse of the Schur complement for the AL preconditioner. This new Schur complement approximation completely avoids the contradictory requirement on the involved parameter while this contradiction is inevitable in the old Schur complement approximation.

To evaluate the new variant of the AL preconditioner, we consider the solution of the linear system obtained at the 30th nonlinear iteration for two cases: laminar and turbulent boundary-layer flow over a flat plate on grids with large aspect ratios. The new variant of the AL preconditioner significantly speeds up the convergence rate of the Krylov subspace solvers for both turbulent and laminar cases. Spectral analysis of the preconditioned systems explains the observed difference. Like the SIMPLE preconditioner, the new AL variant avoids the clustering of the smallest eigenvalues near zero. At the same time, the largest eigenvalues by applying the the new AL variant are significantly smaller than the SIMPLE preconditioner. As a consequence, the new variant of the AL preconditioner outperforms the considered preconditioners in terms of the number of the Krylov subspace iterations.

We present a basic cost model to compare the new variant with others, including the SIMPLE preconditioner which is well established for the RANS equations. The heavier cost of the new AL variant can be payed off with less Krylov subspace

iterations which is seen in this report. However, our test cases so far have been carried out on the modest grid sizes that allow the matrices to be exported and analyzed in Matlab. The future work is planned on the assessment of the new AL variant on larger grid sizes to show the benefit in terms of the reduced total wall-clock time.

Figure 3: Turbulent case: the ten smallest (left) and largest (right) eigenvalues of $\mathcal{P}_{IAL}^{-1}\mathcal{A}_\gamma$ with the new Schur approximation $\widetilde{S}_{\gamma\ \text{new}}$ and different values of γ.

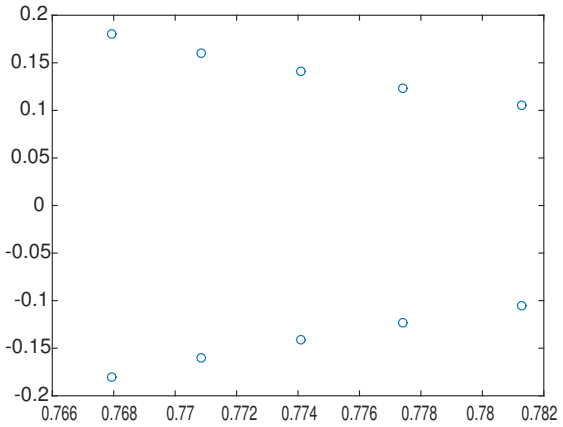

(a) $\gamma = 0.01$

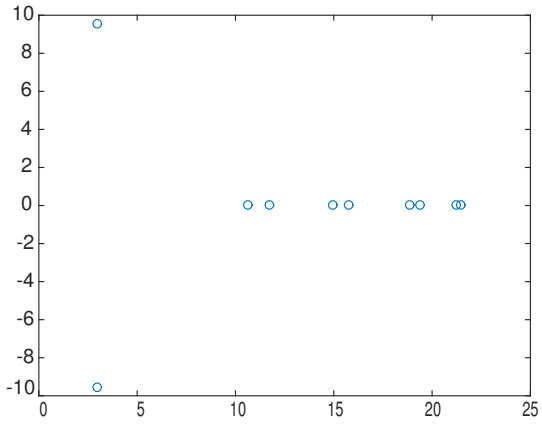

(b) $\gamma = 0.01$

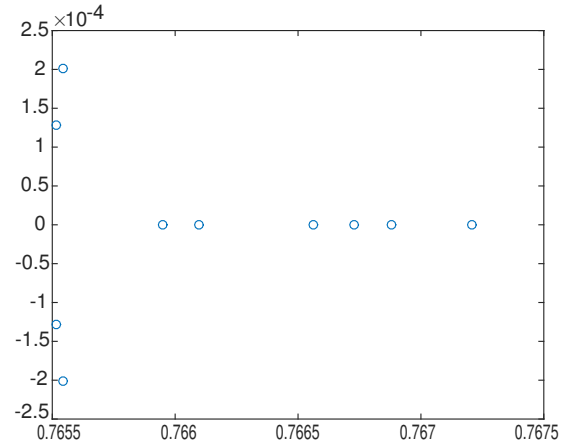

(c) $\gamma = 1$

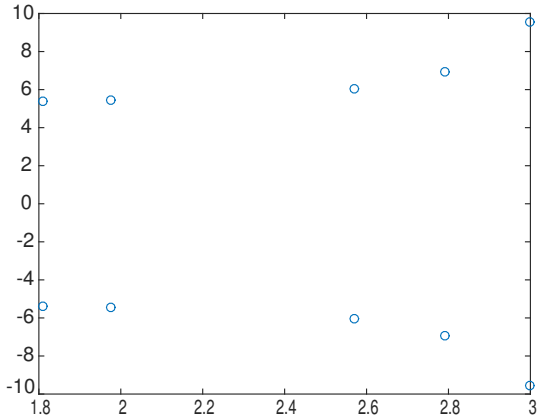

(d) $\gamma = 1$

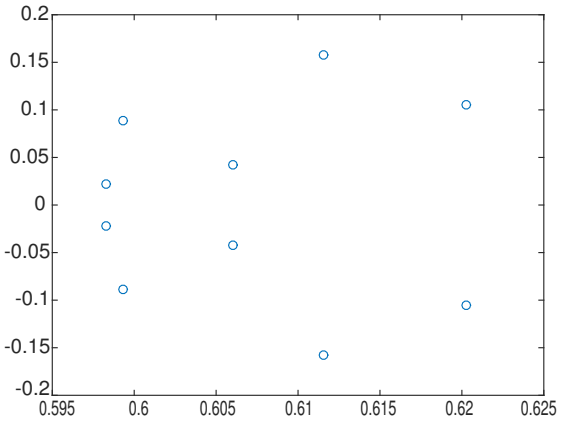

(e) $\gamma = 100$

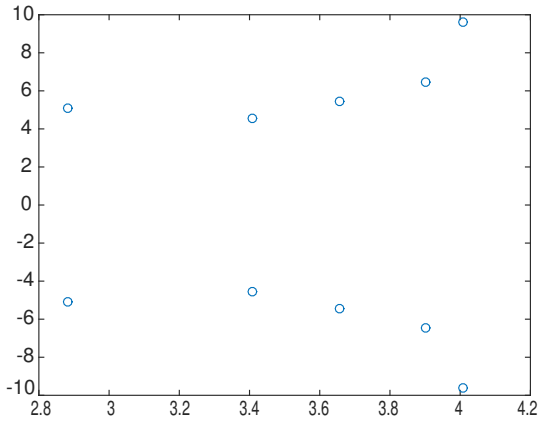

(f) $\gamma = 100$

Figure 4: Turbulent case: the ten smallest (left) and largest (right) eigenvalues of $\mathcal{P}_{MAL}^{-1}\mathcal{A}_\gamma$ with the new Schur approximation $\widetilde{S}_{\gamma\ \text{new}}$ and different values of γ.

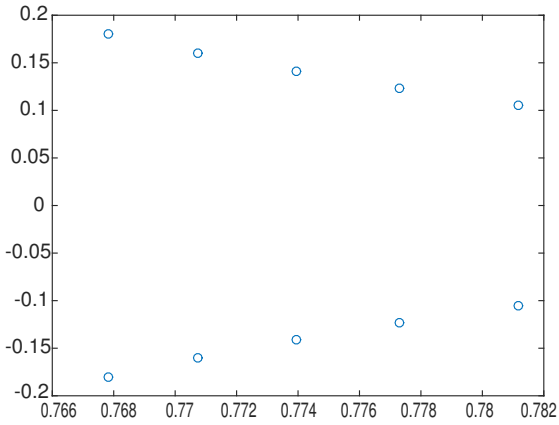

(a) $\gamma = 0.01$

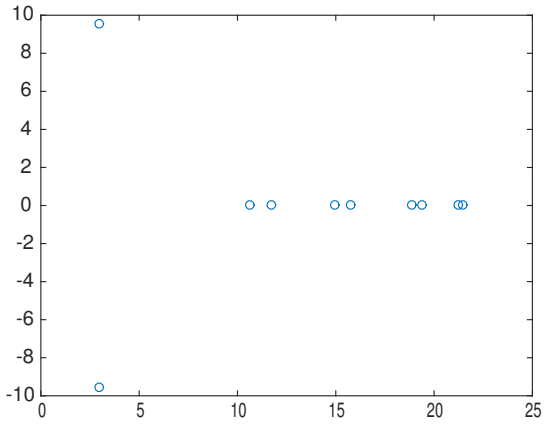

(b) $\gamma = 0.01$

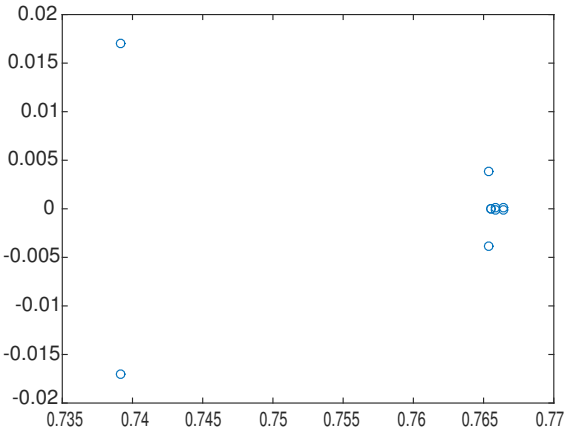

(c) $\gamma = 1$

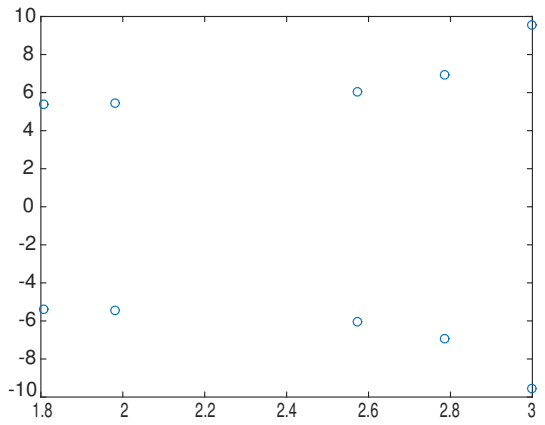

(d) $\gamma = 1$

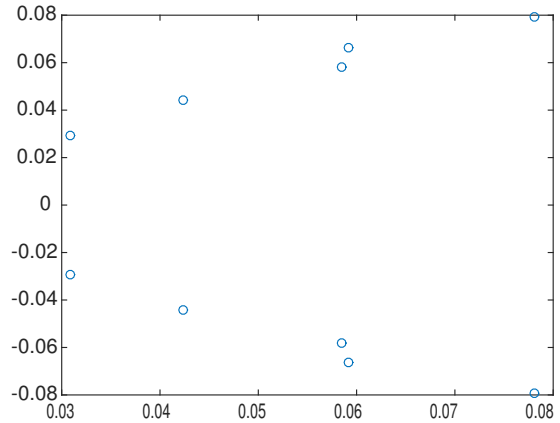

(e) $\gamma = 100$

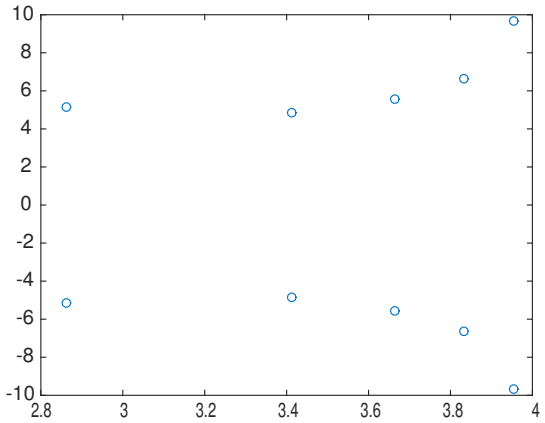

(f) $\gamma = 100$

Figure 5: Turbulent case: the convergence of GMRES (no restart) preconditioned by the ideal and modified AL preconditioner with the new Schur approximation $\widetilde{S}_{\gamma\ \mathrm{new}}$. The involved subsystems are solved directly.

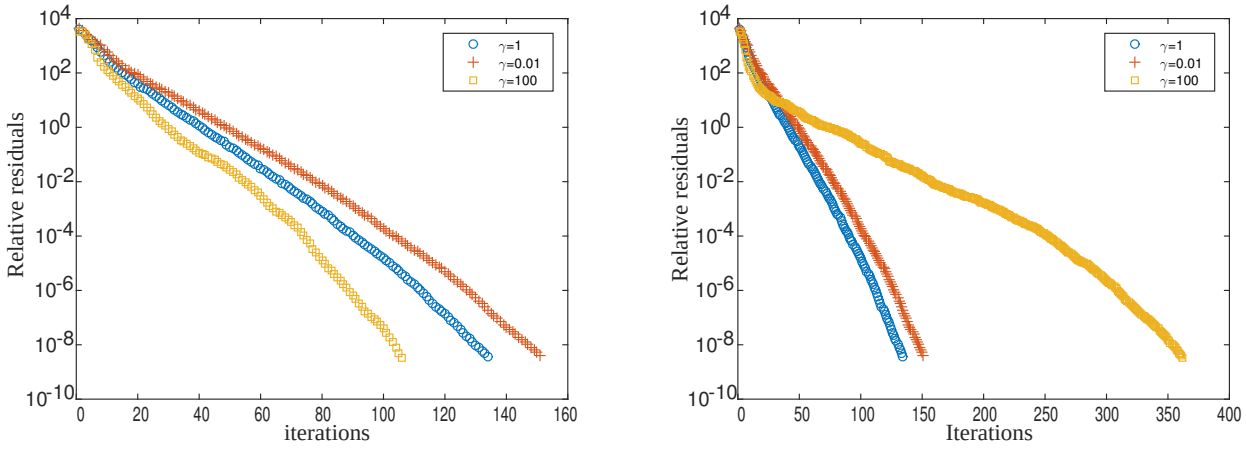

(a) $\mathcal{P}_{IAL}$ (b) $\mathcal{P}_{MAL}$

Figure 6: Turbulent case: the convergence of GMRES (no restart) by using the modified AL preconditioner with the old Schur approximation $\widetilde{S}_{\gamma\ \mathrm{old}}$ and $\gamma = 1$. The involved subsystems are solved directly.

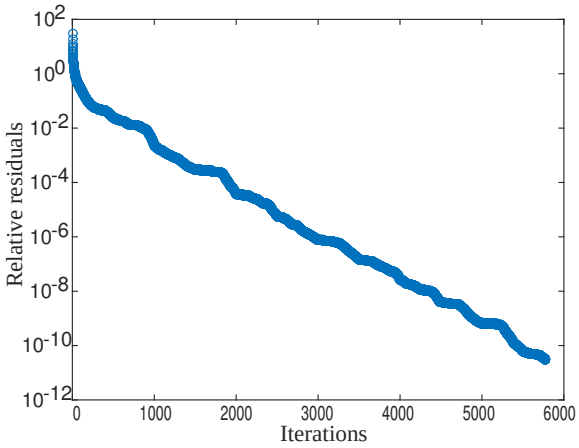

Figure 7: Turbulent case: the ten smallest (left) and largest (right) eigenvalues of $\mathcal{P}_{MAL}^{-1}\mathcal{A}_\gamma$ with the old Schur approximation $\widetilde{S}_{\gamma\ \text{old}}$ and different values of γ.

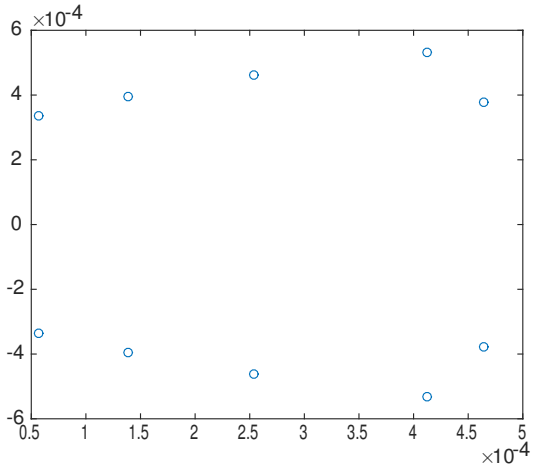

(a) $\gamma = 1$

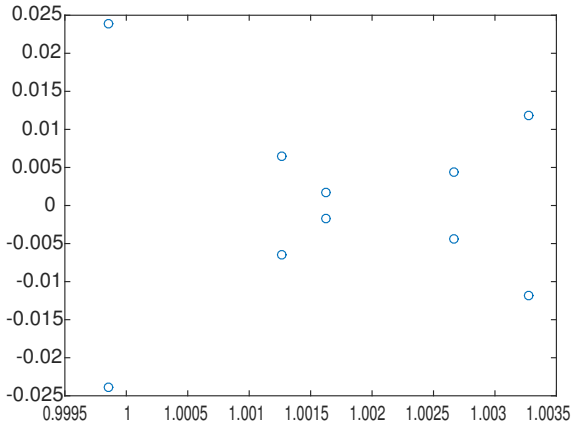

(b) $\gamma = 1$

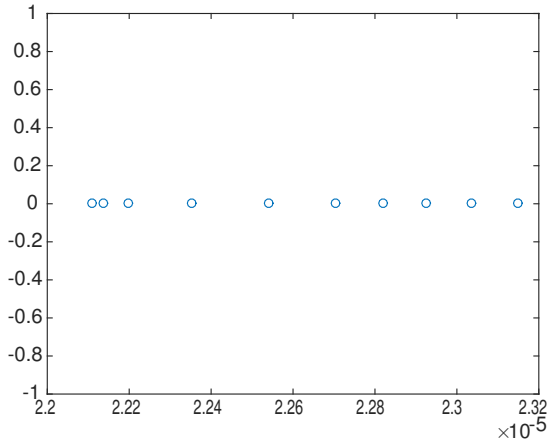

(c) $\gamma = 100$

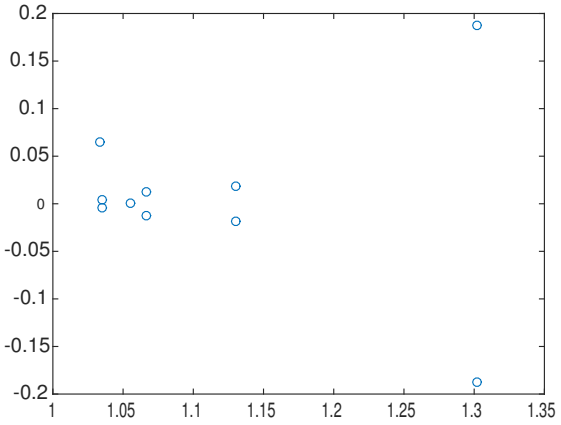

(d) $\gamma = 100$

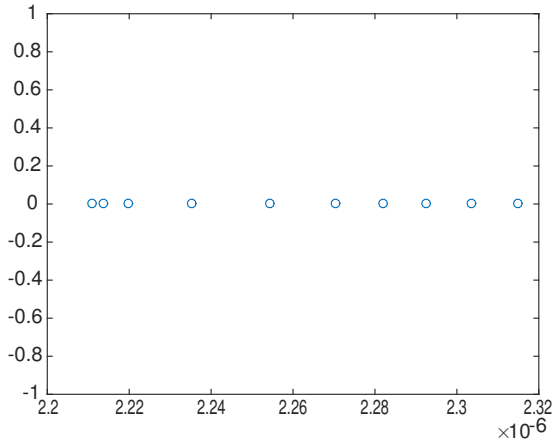

(e) $\gamma = 1000$

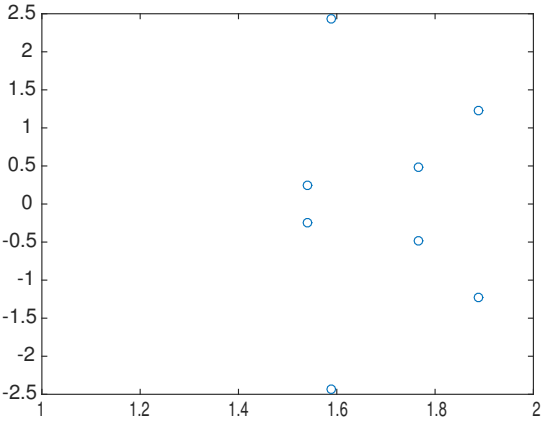

(f) $\gamma = 1000$

Figure 8: Turbulent case: the ten smallest (left) and largest (right) eigenvalues of $\mathcal{P}_{MAL}^{-1}\mathcal{A}_\gamma$ with the new Schur approximation $\widetilde{S}_{\gamma\ \text{new}}$ ($\gamma_{opt} = 1$) and of $\mathcal{P}_{SIMPLE}^{-1}\mathcal{A}$.

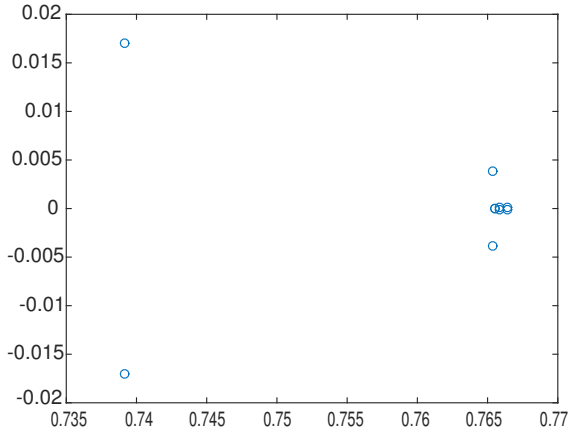

(a) $\mathcal{P}_{MAL}^{-1}\mathcal{A}_\gamma$

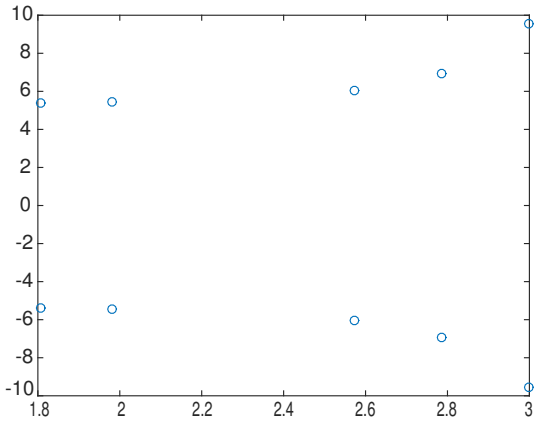

(b) $\mathcal{P}_{MAL}^{-1}\mathcal{A}_\gamma$

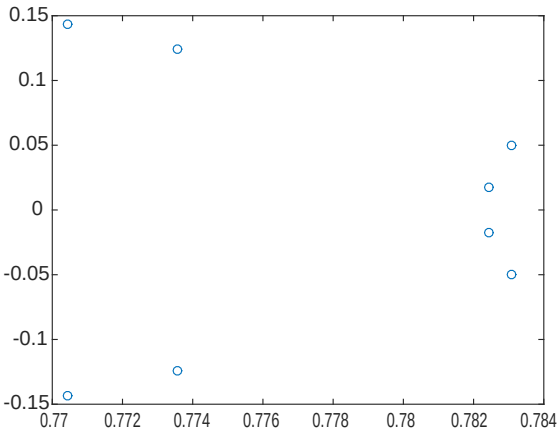

(c) $\mathcal{P}_{SIMPLE}^{-1}\mathcal{A}$

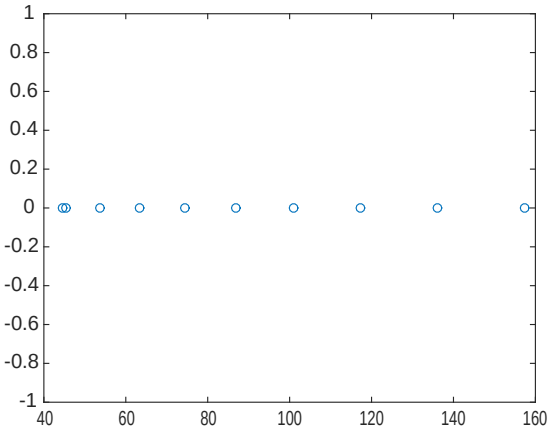

(d) $\mathcal{P}_{SIMPLE}^{-1}\mathcal{A}$

Figure 9: Turbulent case: the convergence of GMRES (no restart) by using the modified AL preconditioner with the new Schur approximation $\widetilde{S}_{\gamma\ \mathrm{new}}$ and the SIMPLE preconditioner. The involved subsystems are solved directly.

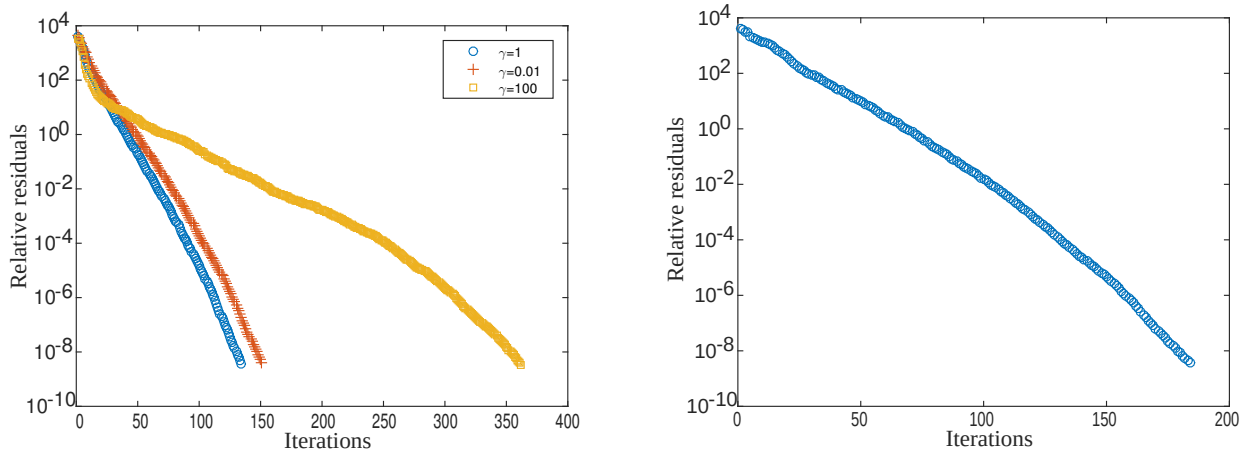

(a) $\mathcal{P}_{MAL}$ (b) $\mathcal{P}_{SIMPLE}$

Figure 10: Laminar case: the ten smallest (left) and largest (right) eigenvalues of $\mathcal{P}_{IAL}^{-1}\mathcal{A}_\gamma$ with the new type Schur approximation $\widetilde{S}_{\gamma\ \mathrm{new}}$ and $\gamma = 1$

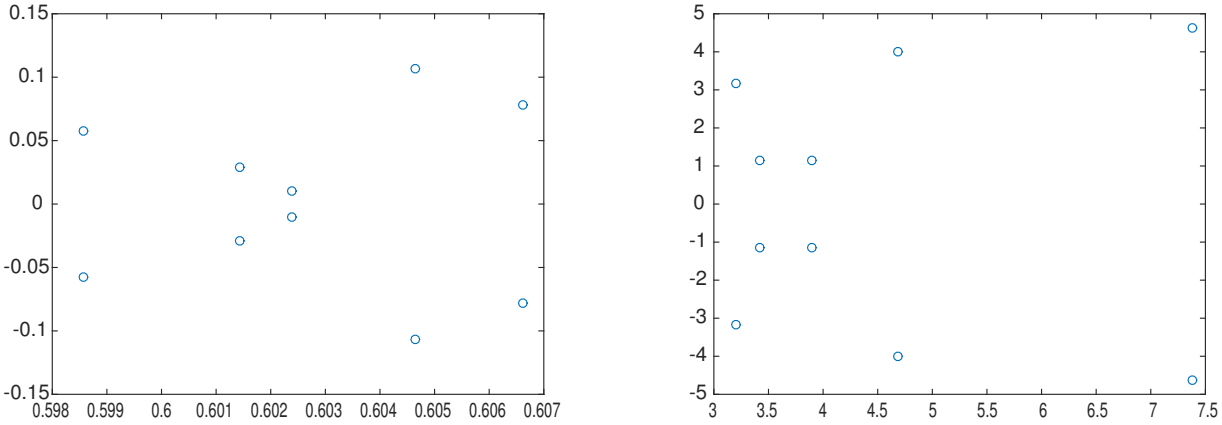

Figure 11: Laminar case: the ten smallest (left) and largest (right) eigenvalues of $\mathcal{P}_{MAL}^{-1}\mathcal{A}_\gamma$ with the new Schur approximation $\widetilde{S}_{\gamma\ \text{new}}$ and different values of γ.

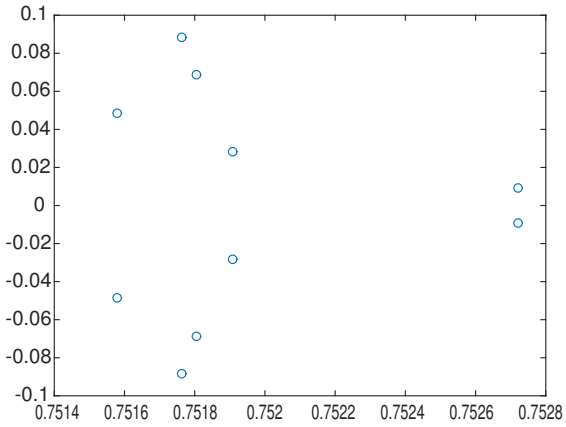

(a) $\gamma = 0.01$

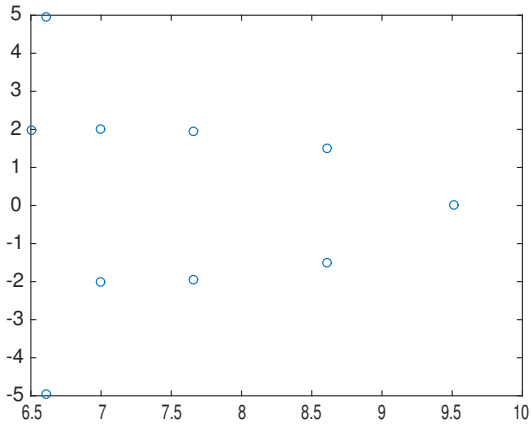

(b) $\gamma = 0.01$

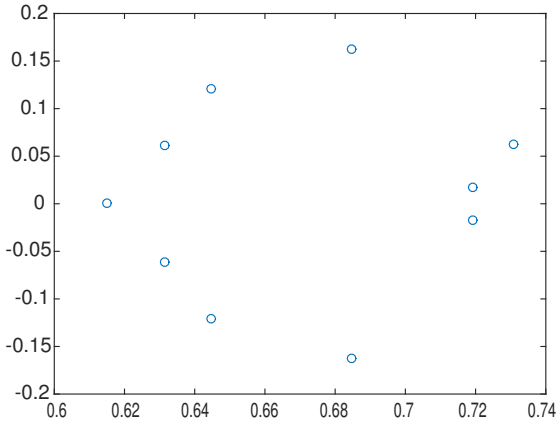

(c) $\gamma = 0.1$

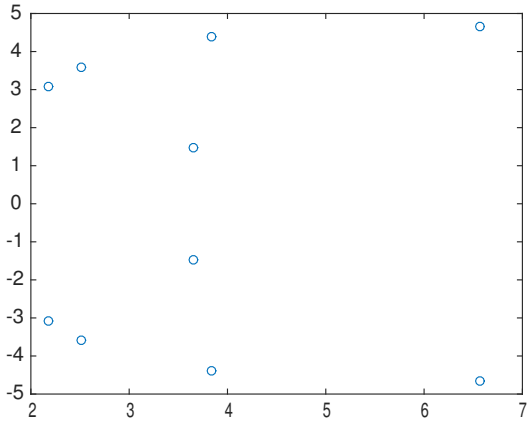

(d) $\gamma = 0.1$

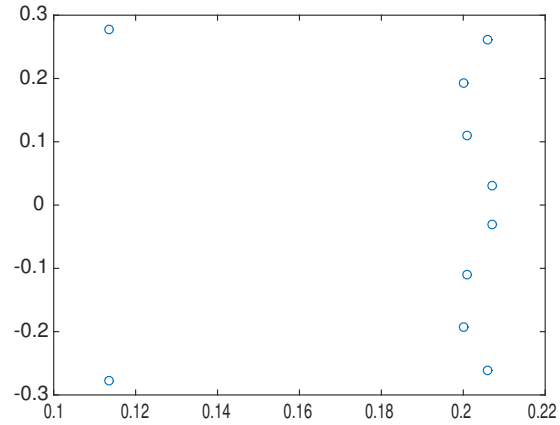

(e) $\gamma = 1$

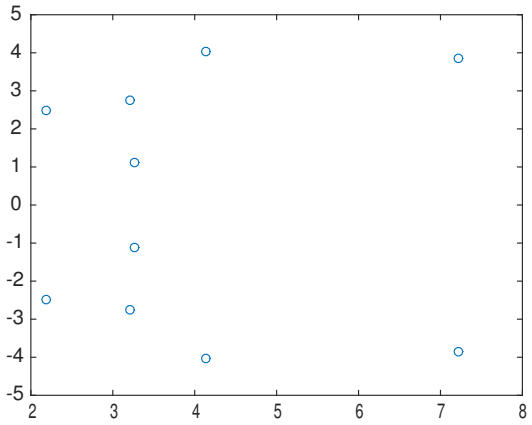

(f) $\gamma = 1$

Figure 12: Laminar case: the ten smallest (left) and largest (right) eigenvalues of $\mathcal{P}_{MAL}^{-1}\mathcal{A}_\gamma$ with the old Schur approximation $\widetilde{S}_{\gamma\ \text{old}}$ and $\gamma_{opt} = 400$ and the new Schur approximation $\widetilde{S}_{\gamma\ \text{new}}$ and $\gamma_{opt} = 0.1$.

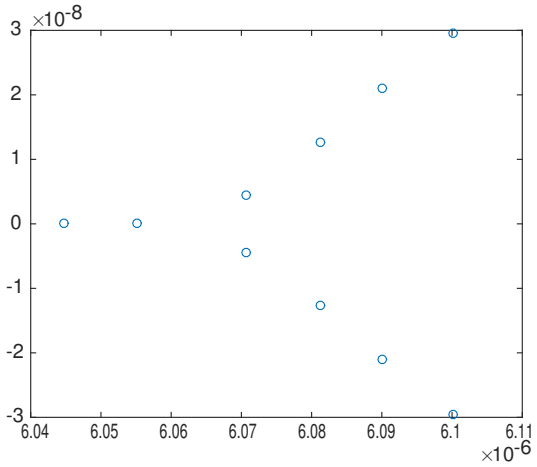

(a) $\widetilde{S}_{\gamma\ \text{old}}$ and $\gamma_{opt} = 400$

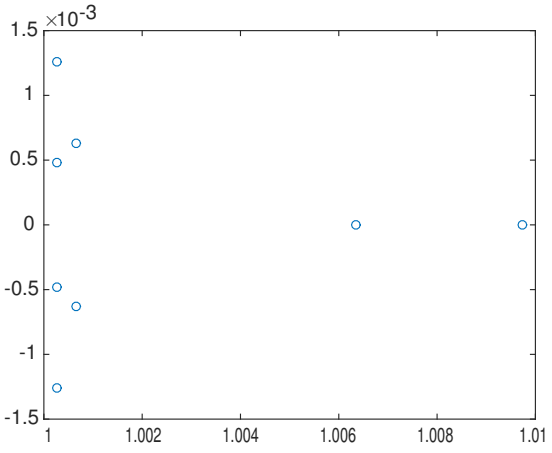

(b) $\widetilde{S}_{\gamma\ \text{old}}$ and $\gamma_{opt} = 400$

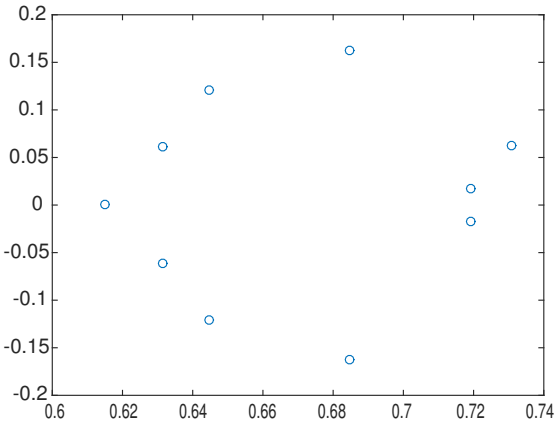

(c) $\widetilde{S}_{\gamma\ \text{new}}$ and $\gamma_{opt} = 0.1$

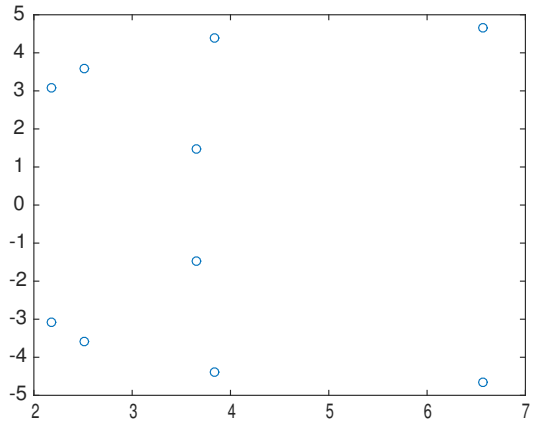

(d) $\widetilde{S}_{\gamma\ \text{new}}$ and $\gamma_{opt} = 0.1$

Figure 13: Laminar case: the ten smallest (left) and largest (right) eigenvalues of $\mathcal{P}_{MAL}^{-1}\mathcal{A}_\gamma$ with the new Schur approximation $\widetilde{S}_{\gamma\ \text{new}}$ ($\gamma_{opt} = 0.1$) and of $\mathcal{P}_{SIMPLE}^{-1}\mathcal{A}$.

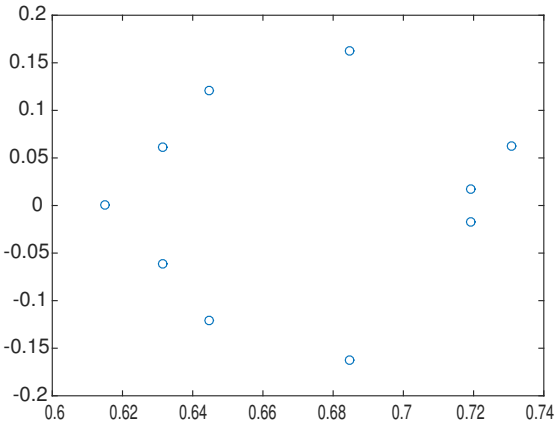

(a) $\mathcal{P}_{MAL}^{-1}\mathcal{A}_\gamma$

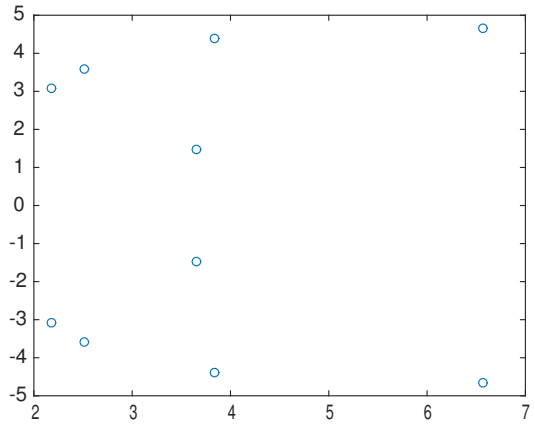

(b) $\mathcal{P}_{MAL}^{-1}\mathcal{A}_\gamma$

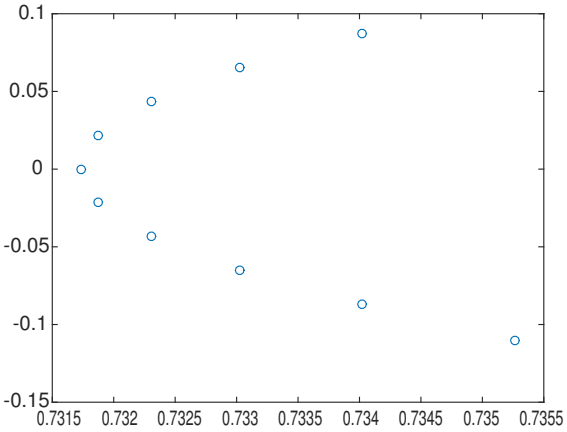

(c) $\mathcal{P}_{\text{SIMPLE}}^{-1}\mathcal{A}_\gamma$

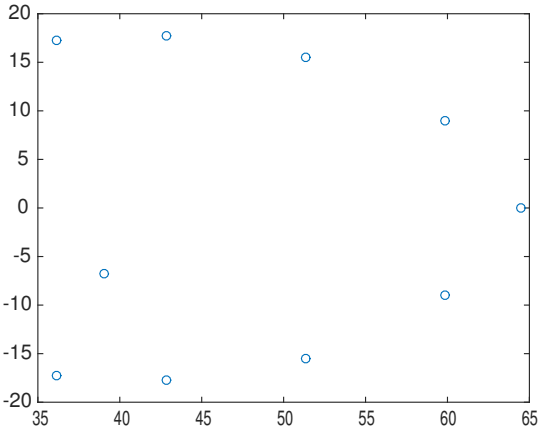

(d) $\mathcal{P}_{\text{SIMPLE}}^{-1}\mathcal{A}_\gamma$

Figure 14: Laminar case: the convergence of GMRES (no restart) by using the modified AL preconditioner with the two Schur approximations and the SIMPLE preconditioner. The involved subsystems are solved directly.

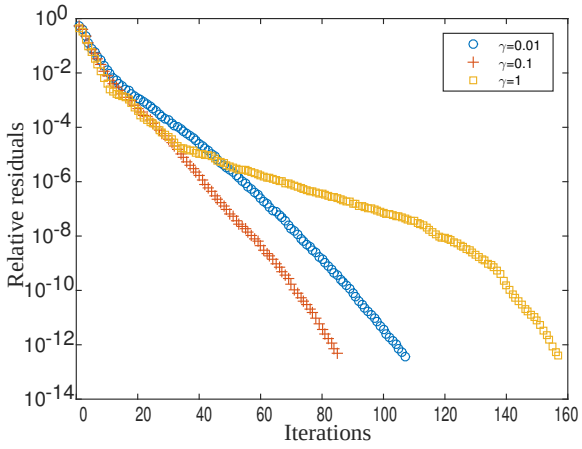

(a) $\mathcal{P}_{MAL}$ with $\widetilde{S}_{\gamma \text{ new}}$

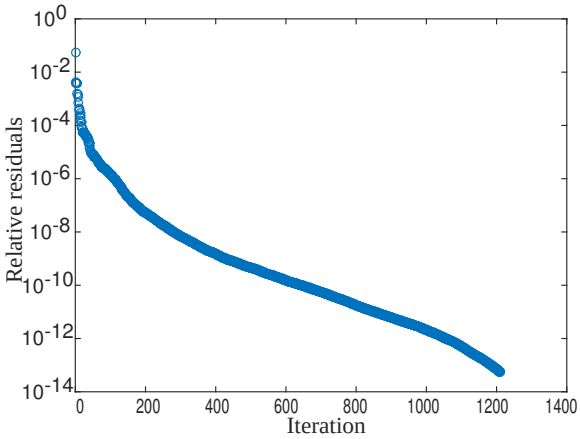

(b) $\mathcal{P}_{MAL}$ with $\widetilde{S}_{\gamma \text{ old}}$ and $\gamma_{opt} = 400$

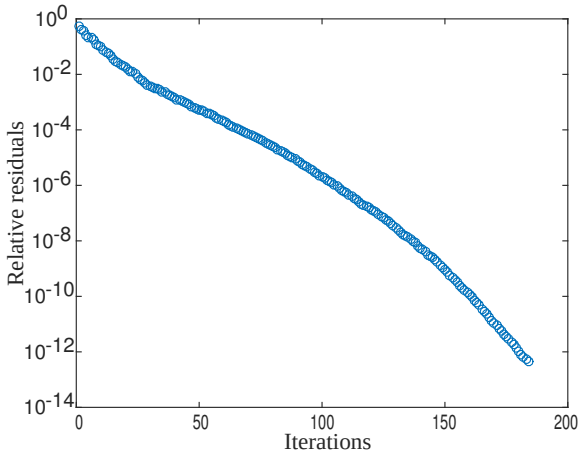

(c) $\mathcal{P}_{\text{SIMPLE}}$

References

[1] M. Benzi. Preconditioning techniques for large linear systems: a survey. *Journal of Computational Physics*, 182:418–477, 2002.

[2] M. Benzi, G.H. Golub, and J. Liesen. Numerical solution of saddle point problems. *Acta numerica*, 14(1):1–137, 2005.

[3] M. Benzi and M.A. Olshanskii. An augmented Lagrangian-based approach to the Oseen problem. *SIAM Journal on Scientific Computing*, 28(6):2095–2113, 2006.

[4] M. Benzi, M.A. Olshanskii, and Z. Wang. Modified augmented Lagrangian preconditioners for the incompressible Navier-Stokes equations. *International Journal for Numerical Methods in Fluids*, 66(4):486–508, 2011.

[5] M. Benzi and Z. Wang. Analysis of augmented Lagrangian-based preconditioners for the steady incompressible Navier-Stokes equations. *SIAM Journal on Scientific Computing*, 33(5):2761–2784, 2011.

[6] M. Benzi and Z. Wang. A parallel implementation of the modified augmented Lagrangian preconditioner for the incompressible Navier-Stokes equations. *Numerical Algorithms*, 64(1):73–84, 2013.

[7] H. Elman, V.E. Howle, J. Shadid, R. Shuttleworth, and R. Tuminaro. Block preconditioners based on approximate commutators. *SIAM Journal on Scientific Computing*, 27(5):1651–1668, 2006.

[8] H. Elman, D. Silvester, and A. Wathen. *Finite elements and fast iterative solvers: with applications in incompressible fluid dynamics*. Oxford University Press, 2014.

[9] J.H. Ferziger and M. Peric. *Computational methods for fluid dynamics*. Springer Science & Business Media, 2012.

[10] D. Kay, D. Loghin, and A. Wathen. A preconditioner for the steady-state Navier-Stokes equations. *SIAM Journal on Scientific Computing*, 24(1):237–256, 2002.

[11] C.M. Klaij. On the stabilization of finite volume methods with co-located variables for incompressible flow. *Journal of Computational Physics*, 297:84–89, 2015.

[12] C.M. Klaij, X. He, and C. Vuik. On the design of block preconditioners for maritime engineering. In M. Visonneau, P. Queutey, and D. Le Touzé, editors, *Proceedings of the Seventh International Conference on Computational Methods in Marine Engineering MARINE*, 2017. May 15 – 17, Nantes, France.

[13] C.M. Klaij and C. Vuik. SIMPLE-type preconditioners for cell-centered, colocated finite volume discretization of incompressible Reynolds-averaged Navier-Stokes equations. *International Journal for Numerical Methods in Fluids*, 71:830–349, 2013.

[14] C. Li and C. Vuik. Eigenvalue analysis of the SIMPLE preconditioning for incompressible flow. *Numerical Linear Algebra with Applications*, 11(5-6):511–523, 2004.

[15] Maritime Research Institute Netherlands. ReFRESCO Web page. `http://www.refresco.org`, 2015.

[16] T.F. Miller and F.W. Schmidt. Use of a pressure-weighted interpolation method for the solution of the incompressible Navier-Stokes equations on a nonstaggered grid system. *Numerical Heat Transfer, Part A: Applications*, 14(2):213–233, 1988.

[17] P. Patankar. *Numerical heat transfer and fluid flow*. McGraw-Hill, New York, 1980.

[18] J. Pestana and A.J. Wathen. Natural preconditioning and iterative methods for saddle point systems. *SIAM Review*, 57(1):71–91, 2015.

[19] D.R. Rijpkema. Flat plate in turbulent flow. , Maritime Research Institute Netherlands, 23279-1-RD, 2009.

[20] Y. Saad. *Iterative methods for sparse linear systems*. SIAM: Philadelphia, PA, 2003.

[21] Y. Saad, Van der Vorst, and A. Henk. Iterative solution of linear systems in the 20th century. *Journal of Computational and Applied Mathematics*, 123(1):1–33, 2000.

[22] A. Segal, M. ur Rehman, and C. Vuik. Preconditioners for incompressible Navier-Stokes solvers. *Numerical Mathematics: Theory, Methods and Applications*, 3(3):245–275, 2010.

[23] D. Silvester, H. Elman, D. Kay, and A. Wathen. Efficient preconditioning of the linearized Navier-Stokes equations for incompressible flow. *Journal of Computational and Applied Mathematics*, 128(1):261–279, 2001.

[24] C. Vuik, A. Saghir, and G.P. Boerstoel. The Krylov accelerated SIMPLE(R) method for flow problems in industrial furnaces. *International Journal for Numerical methods in fluids*, 33:1027–1040, 2000.

[25] P. Wesseling. *Principles of computational fluid dynamics*. Springer Science & Business Media, 2009.

[26] F.M. White. *Fluid mechanics*. McGraw-Hill, 1994.

[27] X.He, C.Vuik, and C.M.Klaij. Block-preconditioners for the incompressible Navier-Stokes equations discretized by a finite volume method. *Journal of Numerical Mathematics*, 25(2):89–105, 2017.